Influences of the Co content and of the level of high temperature on the microstructure and oxidation of cast Ni, Co-based Cr-rich TaC- containing cast alloys

Patrice Berthod, Zohra Himeur, Pierre-Jean Panteix

Influences of the Co content and of the level of high temperature on the microstructure and oxidation of cast {Ni, Co}-based Cr-rich TaC-containing cast alloys

Patrice Berthod, Zohra Himeur, Pierre-Jean Panteix

Institut Jean Lamour (UMR 7198), department CP2S
Faculty of Sciences and Technologies, University of Lorraine
BP 70239, 54506 Vandoeuvre-lès-Nancy – France

Corresponding author's e-mail: patrice.berthod@centraliens-lille.org
Corresponding author's phone: (33)3 8368 4666 and fax number: (33)3 8368 4611

Abstract

A series of six alloys derived from a Ni-25Cr-0.4C-6Ta (wt.%) base one was developed by substituting nickel by cobalt. They were synthesized by casting and exposed to oxidative environment at two high temperatures. Their bulk microstructures were studied in as-cast condition and in two high temperature aged states. Their surfaces after oxidation during aging were characterized. The cobalt enrichment succeeded in avoiding chromium carbides formation and in stabilizing the TaC carbides at high temperature. As the high temperature morphologic stability of TaC was not perfect, it was much better than the one of the chromium carbides, but can be improved by the total removal of nickel. Unfortunately, at the same time, the oxidation behavior, initially good, shows increased rate of the oxides formation. The room temperature hardness was also significantly increased by the substitution of Ni by Co, and decreased after aging when carbides became rounder or fragmented.

Keywords: Cast superalloys; Nickel; Cobalt; Tantalum Carbides; Microstructure; High temperature oxidation;

1. Introduction

In parallel with many totally different applications such as medical ones [1], nickel-based superalloys have been used for many years in components working at high temperature [2]. Among them the ones able to be exploited at very high temperature are surely the single-crystalline ones [3,4]. These ones demonstrate superior behavior in very hot conditions in oxidative environment, even if their microstructures tend to evolve during exposure to high temperature with simultaneous application of mechanical stresses [2,3,5,6]. On the other hand, here too in parallel with many other applications such as prosthetic ones [7] or cutting tools [8], another important family of superalloys is constituted of the cobalt-chromium alloys, prepared by casting processes followed by forging or not [9]. Cobalt-based alloys rich in chromium can be met as constitutive materials of aeronautical components working at high temperature, but also in the glass industry [10], for example.

In such nickel-based or cobalt-based alloys high mechanical strength may be achieved at elevated temperature following different ways, for example by gamma prime precipitates for the single-crystalline Ni alloys or by solid solution strengthening for the Co alloys. However, in both cases, significant reinforcement may also be obtained by taking benefit from dispersed hard particles as carbides [2,3]. Particularly efficient carbides for elevated temperatures of work are tantalum carbides, which may precipitate during solidification (primary carbides) or thanks to judicious heat treatment (secondary carbides). Their very interesting script-like shape inherited from solidification and their rather high temperature morphological stability allows high performances in term of creep resistance at high temperature. For example some polycrystalline cobalt-nickel superalloys rich in chromium and containing TaC as single carbide, are successfully used at temperatures of 1200°C and more. Lifetimes of several hundreds of hours can be reached under constant tensile stresses (several tens of MPa) in severe conditions of oxidation by gases and of corrosion/erosion by melts [10]. The formation of TaC logically requires the presence of carbon and of tantalum, the latter one being also able to act as a solid solution strengthener. It is also known to influence the high temperature behavior of refractory alloys in the microstructure stability field [3, 11] or in the hot oxidation one [12, 13].

When the alloy must contain high quantity of chromium to well resist to high temperature oxidation and corrosion, tantalum carbides can be difficult to obtain. This seems to depend on the base element as seen earlier in 30wt.%Cr-containing cast alloys based on Co, Fe or Ni [14-16], for instance. TaC easily appeared during solidification in {Co-30Cr, wt.%}-based [14] and {Fe-30Cr, wt.%}-based [15] alloys and were thereafter stable during exposure at high temperature, while it was all the contrary in {Ni-30Cr, wt.%}-based alloys [16]. The TaC which can be obtained without any problem cannot significantly reinforce Fe-based alloys rich in chromium, since the Body Centered Cubic matrix of these alloys is much too weak to allow any benefit from the presence of TaC carbides. Co-based alloys take benefit from both the intrinsic high mechanical strength of their matrix and the stable TaC carbides, but they are often hard to machine at room temperature. This difficulty is enhanced by the presence of the tantalum carbides. In addition their behavior in oxidation at high temperature is far from perfect. Indeed they are often threatened by the appearance, in addition to Cr_2O_3 (chromia), of $CoCr_2O_4$ spinel oxide and of the CoO cobalt oxide, both not protective and leading to the loss of the chromia-forming behavior. Nickel-based alloys rich in chromium appear as being a good compromise of reasonable high temperature strength and satisfying oxidation behavior. But their high temperature mechanical properties cannot be improved by TaC carbides as efficiently as for cobalt-base alloys. Inspired by what was observed in the case of addition of sufficiently high content in iron to nickel-chromium alloys [17], as is to say the stabilization of TaC carbides with favorable fractions and morphologies, one can think to apply this principle to cobalt.

In this work cobalt was effectively added to a {Ni(bal.)-25Cr-0.4C-6Ta, wt.%}-base. The effect of such additions on the TaC fractions obtained during solidification was observed. The hardness at ambient temperature, the TaC characteristics after exposure at two different high temperatures and the apparent behavior in oxidation at high temperature were characterized.

2. Experimental details of the study

2.1. Choice and synthesis of the alloys

A series of six alloys was chosen for the study. From an initial base consisting of the Ni(bal.)-25Cr-0.4C-6Ta (wt.%) alloy, a second alloy was defined by replacing a fifth of the nickel quantity by the same amount of cobalt. A third alloy was derived from the second one by replacing a second fifth of the initial nickel quantity, again by the corresponding amount of cobalt… and so on until finishing with a sixth alloy based only on cobalt. These six alloys were named “5Ni0Co”, “4Ni1Co”. “3Ni2Co”, “2Ni3Co”, “1Ni4Co” and “0Ni5Co” respectively. Their theoretical compositions are given in Table 1.

The alloys were elaborated by using a CELES high frequency induction furnace. Appropriate amounts of pure elements (Alfa Aesar, purity > 99.9%) were first weighed using a precision balance, to have finally about 40 grams of each of the six alloys. These parts of pure elements were placed in the metallic crucible of the furnace (copper made, cooled by internal circulation of water during operation). A silica tube was placed around to isolate the fusion chamber from the laboratory air. Pumping was carried out until obtaining about 5×10^{-2} millibars as internal pressure. Vacuum was done again and pure argon was injected until reaching 800 millibars. Pumping until 5×10^{-2} millibars was then done again. After three cycles an internal atmosphere of about 300 millibars Ar was obtained. Heating was carried out by injecting the 100 kHz alternative current corresponding to 2500 Volts. After thermal homogenization voltage was increased to reach 4000 Volts and was then maintained for three minutes at this value. Cooling down to room temperature was followed by a second thermal cycle, identical to the first one, in order to ensure the melting of all solids and good homogenization of the melt before final solidification and cooling.

2.2. Ingot cutting, sample preparation, high temperature exposures

Each obtained ingot was cut using a Buelher Delta Abrasimet metallographic saw. Four quarters were thus obtained.

One was kept for preparing a metallographic sample devoted to the examination and characterization of the microstructure of the alloy in its as-cast state. For that this first quarter was cut again, in two parts. These parts were embedded in a cold resin mixture (ESCIL) and ground. This was done using paper from 120-grit to 1200-grit, in water. After washing and ultrasonic cleaning, samples were polished using textile disk containing 1µm hard particles until a mirror-like surface state was obtained.

Two other quarters were considered for the exposure at high temperature in a Nabertherm muffle furnace: one at 1127°C for 24 hours, and the other one at 1237°C for 24 hours (measured temperatures). After high temperature exposure they were ground with papers up to 1200-grit, with smoothing of the edges. Gold was cathodically deposited all around the oxidized samples in order to obtain electrical conductivity of the surface despite the presence of oxides, and thus to allow subsequent nickel electrolytic deposition. The gold-coated high temperature aged samples were covered all around by a sufficiently thick nickel layer to protect the oxide scales from deterioration during cutting. The parameters of this electrolytic deposition were: Watt’s

bath maintained at 50°C, current density: 1.6 A/dm², duration: at least two hours. Careful cutting in two halves was achieved using the Buehler Delta Abrasimet saw again, and these two halves were prepared as earlier described for the samples for as-cast microstructure examination.

2.3. Bulk microstructure and oxidized surfaces examinations, hardness measurements

The bulks of the six alloys in their as-cast state and in their two aged states were examined by scanning electron microscopy (SEM: JEOL JSM6010LA) in back scattered electrons mode (BSE). The chemical compositions were controlled using the Energy Dispersive Spectrometry device (EDS) equipping the SEM and spot analyses were tried on the seen particles. For each alloy and each metallurgical state three ×1000 SEM/BSE micrographs were subjected to image analysis (Photoshop CS software) to evaluate the surface fractions of the different phases.

The cross-sectional samples prepared from the aged alloys were examined to characterize the formed oxidation products and the subsurface changes. The oxides were specified by EDS analysis and, when possible (i.e. when allowed by a not too severe oxide spallation during cooling), the thickness of the external oxide scales was measured in several locations. The depth from the alloy/scale interface in which carbides have disappeared was also measured, in several locations too. To understand the apparent oxidation behaviour the chemical composition in alloy very close to the alloy/scale interface was measured by EDS spot analysis.

The hardness of the as-cast alloy and its two versions aged at 1127°C or 1237°C was measured by indentation using a Testwell Wolpert apparatus. The Vickers method was chosen, and the applied load was 10 kg. Five indentations per sample were carried out.

3. Results

3.1. Qualitative bulk examinations

The microstructures of the six alloys were studied for their three metallurgical states: as-cast, after aging at 1127°C and after aging at 1237°C. To facilitate the comparison between these different states representative SEM/BSE micrographs (magnification: ×1000) are presented together in Fig. 1 for the “5Ni0Co” alloy, in Fig. 2 for the “4Ni1Co”, in Fig. 3 for the “3Ni2Co” alloy, in Fig. 4 for the “2Ni3Co”, in Fig. 5 for the “1Ni4Co” alloy and in Fig. 6 for the “0Ni5Co”.

On these micrographs it first can be observed that all alloys started their solidification by the development of dendrites of matrix and finished it by the eutectic precipitation of matrix + carbides mix. The carbides are present only in the interdendritic spaces, in the as-cast alloys. These carbides can be of two types which were subjected to EDS analyses. Despite that they were generally too small to be analyzed using this technique, the results obtained on the coarsest carbides suggest that the black particles are really chromium carbides, with stoichiometry close to Cr_7C_3. Due to the uncertainty about the exact stoichiometry, it was preferred to simply note these phases as “Cr_xC_y”. The white particles are TaC carbides. The same particles are

observed in the aged alloys but one can also remark that their morphology and location may have changed.

Concerning the as-cast microstructures it appears judicious to allocate the six alloys into three groups: a first one gathering the two Ni-richest alloys (“5Ni0Co” and “4Ni1Co”) which contain chromium carbides and tantalum carbides in equivalent quantities, the second one consisting in the two alloys with almost equivalent quantities in Ni and Co (“3Ni2Co” and “2Ni3Co”) which contain mainly tantalum carbides but also a little part of chromium carbides, and the third one concerning the two Co-richest alloys (“1Ni4Co” and “0Ni5Co”) in which only tantalum carbides are present.

The three groups also exhibit different microstructure evolution during aging. The alloys of the first group remain with the two types of carbides after the isothermal stage, whatever the aging temperature is. But their shapes significantly evolved as coarsening of the chromium carbides and fragmentation/coarsening for the tantalum carbides are observed. These changes are more marked after heat-treatment at 1237°C than at 1127°C. The two alloys of the second group are less affected by the coarsening and fragmentation phenomena. In as-cast state they mainly contain TaC carbides and these ones seem to be less fragmented and coarsened than the two previous alloys, even after aging at the highest temperature. The chromium carbides, initially in low quantities in the as-cast microstructures are still present after aging, whatever the temperature is, and their morphologies did not seemingly evolve. Another difference with the first group is the higher tendency to precipitate numerous little secondary tantalum carbides during aging, especially when the aging temperature is 1127°C. After aging at 1237°C it seems that the TaC precipitate in the matrix are less numerous and with a greater size. Concerning the alloys of the third group, fragmentation occurred again (in higher proportions for the “1Ni4Co” alloy than for the other one) but with less coarsening of both primary and secondary tantalum carbides. Secondary TaC precipitation and coarsening were obviously hindered for the “0Ni5Co” alloy while the two phenomena are more visible for the “1Ni4Co” alloy. This is observed for the two aging temperatures.

3.2. Quantitative microstructure analysis; results of indentation

The surface fractions of the chromium carbides and of the tantalum carbides were measured on three ×1000 SEM/BSE pictures taken in zones randomly chosen in the bulk of the metallographic samples, using an image analysis tool of the Photoshop CS software of Adobe. This was done for all alloys for their three metallurgical states. The obtained results are displayed in Table 2 and their evolution versus the alloy chemical composition illustrated in Fig. 7. After having confirmed that the chromium carbides surface fraction really decreases when substitution of nickel by cobalt is increasing, it can be noticed that the quantity of chromium carbides tends to become higher during aging (Fig. 7 A). Furthermore it increases when the aging temperature increases. Concerning the tantalum carbides (Fig. 7 B), the results globally confirm that the TaC surface fraction increases when the substitution of nickel by cobalt is greater. The results concerning the 1127°C-aging are rather scattered, which does not reveal any clear dependence of the TaC fraction on the Co content. In contrast there is a very regular increase of the TaC fraction versus the Co content after 1237°C-aging. Despite

the rather curious results obtained for 1127°C, it seems that aging at high temperature induced an increase in TaC quantity for all alloys.

For all alloys and their three metallurgical states five Vickers indentations under a 10kg-load were carried out. The obtained values are displayed in Table 3 and their evolution versus the chemical composition of alloy is illustrated in Fig. 7 C. These graphs clearly show a hardness increase when the Co-substitution of Ni is greater, this for all states (as-cast or aged). Knowing that cobalt is intrinsically harder than nickel, it appears rather logical to observe an increase in hardness when progressively moving from a nickel base to a cobalt one. Globally the alloys tend to be less hard after aging than before. This difference in hardness is more visible between the as-cast alloys and the 1237°C-aged ones, this seeming to point out an effect of the coarsening of the chromium carbides and of the fragmentation + coarsening of the TaC. One can notice that the intermediate alloys ("2Ni3Co" and "3Ni2Co") tend to be a little harder after 1127°C-aging than in their as-cast condition and in their 1237°C state: this may point out a strengthening effect of the numerous secondary carbides precipitated in matrix during the 1127°C exposure.

3.3. *Qualitative cross-sectional examinations*

The surface (and subsurface) states of the six alloys aged at 1127°C and aged at 1237°C were characterized on the same cross-sectional samples as previously. Again, to facilitate the comparison between these different states per alloy representative SEM/BSE micrographs (magnifications: ×250 and ×1000) are presented together in Fig. 8 for the "5Ni0Co" alloy, in Fig. 9 for the "4Ni1Co", in Fig. 10 for the "3Ni2Co" alloy, in Fig. 11 for the "2Ni3Co", in Fig. 12 for the "1Ni4Co" alloy and in Fig. 13 for the "0Ni5Co".

The surface and subsurface behavior of all alloys, for all temperatures, can be described as follows:

- oxidation took place externally with the formation of an outer continuous oxide scale covering the alloy, involving chromium and also possibly the base elements
- oxidation also occurred internally with appearance of $CrTaO_4$ oxides in the subsurface close to the alloy/external oxide scale interface
- carbides of all natures (Cr_xC_y, TaC) and all origins (primary or secondary) disappeared over a depth of several tens of micrometers. They are present again deeper.

Considering the high temperature oxidation point of view the six alloys may be gathered into groups. The first group, including the three nickel-richest alloys ("5Ni0Co", "4Ni1Co" and "3Ni2Co"), corresponds to the outer presence of a Cr_2O_3 (chromia) scale, unfortunately lost during cooling in some cases (1237°C); when observable, this oxide is obviously compact and efficiently protected the alloys from too rapid and general oxidation. The second group, containing the three cobalt-richest alloys ("2Ni3Co", "1Ni4Co" and "0Ni5Co"), is distinguished by the deterioration of the chromia scale (irregular, presence of porosities) and/or the upcoming loss of the chromia-forming behavior (presence of nickel and/or cobalt oxides).

3.4. Quantitative metallographic results about oxidation

After these first observations, the thickness of the external scale was measured in about five different locations on the cross-sections, as well as the depth of the carbide-free zone. The results are displayed in Table 4 and plotted versus the chemical composition of the alloy in Fig. 14 (Fig. 14 A for the oxide scale thickness and Fig. 14 B for the carbide-free depth). To complete the observations concerning the lasting quality or inversely the imminence of the loss of the chromia-forming behavior, three to five spot EDS measurements of the local chemical composition of the alloy were performed close to the oxidation front. The results are displayed in Table 5 and plotted versus the alloy chemical composition in Fig. 14 C).

It appears that the oxide scale thickness increases with the Ni by Co substitution in alloy and with the temperature. For the first point, no evolution may be noticed as long as nickel remains the major element (from “5Ni0Co” to “3Ni2Co”), but the oxide thickness dramatically increases when the alloy contains more cobalt than nickel. The evolution of the carbide-free depth seems being inversed, notably at 1237°C. Indeed, by adding cobalt the carbide-free zone decreases in depth until cobalt becomes more present than nickel. The carbide-free depth becomes stabilized for further cobalt increases. Concerning the samples aged at 1127°C, the evolution is not so monotonous. Furthermore the three nickel-richest alloys seem to exhibit carbide-free zones a little thinner than the three cobalt-richest ones. The evolution of the chromium content in extreme surface versus the Co content in the alloy is the same for the two temperatures: it regularly decreases between the alloy only based on nickel and the alloy only based on cobalt.

4. Discussion

For 25Cr, 0.4C and 6Ta (wt.%), whatever the Co/Ni balance for the base element is, the obtained alloys all contain, in the as-cast condition, a dendritic matrix and primary carbides on a eutectic nature and located in the interdendritic spaces, without any other particle/phase such as pre-eutectic carbide for example. A microstructure thus constituted of imbricated matrix dendrites and carbides closely mixed with the periphery of these dendrites is favorable to high mechanical properties at elevated temperature. Unfortunately the morphology of the carbides evolves rapidly at high temperature, faster for 1237°C than for 1127°C, faster for chromium carbides than for tantalum carbides and, for the later ones, faster when the matrix is rich in nickel than when it is rich in cobalt. When initially present, as is to say when the alloy is richer in nickel than in cobalt, the chromium carbides coalesce and become coarser and rounder. The tantalum carbides become fragmented into alignments of round carbides. This firstly resulted in a decrease of room temperature hardness for all alloys, from initial hardness levels which become higher when cobalt substitutes more nickel in the alloy. Secondly, this reveals highly probable mechanical weakening of the alloy at high temperature.

The tendency to coarsening or fragmentation of the carbides may be easily explained by the thermodynamic reduction of the alloy energy due to the decrease of the cumulative matrix-carbides interface area. After 24 hours of exposure at 1127°C this

morphologic evolution is not sensibly advanced but some first little changes can be observed. It can be assumed that the carbides morphology is significantly transformed after much longer exposure. Fragmentation and/or coarsening occurred faster at 1237°C, with significant modifications after only 24 hours. Since this affects essentially the nickel-richest alloys specifically for their chromium carbides, it clearly appears that these alloys can be expected to be used under stress only at 1100°C and lower temperatures than at around 1200-1250°C. At this later temperature the cobalt-richest may be still usable. The intermediate alloys, containing almost cobalt as much as nickel, seem to be the best candidates to resist mechanical stresses and creep at around 1100-1150°C. Indeed, their primary carbides (all of tantalum) are almost unaffected, and they exhibit particularly dense and homogenous fine TaC carbides in the matrix, which obviously precipitated spontaneously during the 24 hours at 1127°C.

So, concerning the bulk microstructure, it can be concluded that progressively substituting nickel by cobalt has a triple effect: (i) hardening the matrix, (ii) replacing the part of primary carbides which were initially chromium carbides by more morphologically stable TaC carbides, and stabilizing at high temperature the morphology of TaC carbides which were already more stable than the chromium carbides. On the microstructure point of view, and consequently for the resulting mechanical properties, the temperature at which the M-25Cr-0.4C-6Ta alloy may be usable under stresses increases of about one hundred Celsius degrees.

Concerning the behavior in high temperature oxidation the evolutions of the three considered parameters (oxide scale thickness, subsurface carbide-free depth, chromium content in extreme surface) are consistent and demonstrate a significant decrease in oxidation resistance by replacing nickel by cobalt. By crossing the {Co=Ni} limit the external scale becomes clearly deteriorated in quality (porosity) and purity (not only chromia but additional presence of cobalt oxide). Due to the poorer protection of alloy, oxidation becomes faster, this resulting in thicker external oxide. In the same time the chromium diffusion in the bulk becomes more difficult, and its diffusivity decreases with the progressive replacement of the nickel-based matrix by a cobalt-based ones. This limits the depth of alloy supplying the oxidation front in Cr: chromium carbide-free zone is not so deep, and a more intensive solicitation of the thinner outer part of the alloys involves locally low chromium contents. Tantalum and tantalum carbides are also concerned: indeed, for the nickel-richest alloys, the limit between the carbide-free zone and the inner part of alloy still containing TaC carbides obviously corresponds to the same concerning chromium and the chromium carbides. When TaC are the single carbides initially present (i.e. case of the cobalt-richest alloys) the tendency goes on: the limit between alloy with TaC and the carbide-free zone progressively approaches the oxidation front although the oxidation of tantalum in subsurface seems to increase (seemingly more $CrTaO_4$ oxides). Diffusion of tantalum to meet oxygen diffusing in the alloy in the other direction seems then more difficult. This double increasing difficulty for Cr and Ta to diffuse through the matrix more and more enriched in cobalt (to the detriment of nickel) appears to be the origin of the lower oxidation resistance (Cr) but also of the persistence of an interdendritic network of TaC still close to the surface and favorable to a mechanical resistance of this outer zone of the alloy.

5. Conclusion

By exploring the as-cast microstructures, the microstructures aged at different high temperatures, the evolution of the corresponding room temperature hardness and by having a look at the oxidized states after aging treatment, this work pointed out several significant consequences of the progressive substitution of the base element by cobalt until total replacement in an initial chromium-rich nickel-based alloy containing carbon and tantalum in equivalent atomic quantities. As expected this evolution of chemical composition had positive effects (chromium carbides deleted in the microstructure and simultaneous increased TaC densities, progress in carbide stability at high temperature, potentially better mechanical behavior at high temperature) but also negative ones (increase of hardness and probably lower machinability, deterioration of the high temperature oxidation behavior). After these first observations and the consequent hypothesis, further work may consist in really characterizing the high temperature mechanical behavior of this series of alloys, as well as longer exposures at high temperatures, to confirm the tendencies revealed here about the bulk microstructures changes and the transition from good behavior to catastrophic oxidation. Fortunately, it remains possible to enrich in chromium the surface and subsurface of the alloys containing TaC as single carbide, by using pack-cementation. Indeed it was demonstrated that such coating operation may be successful for polycrystalline cast cobalt-nickel containing only TaC [18, 19]. Thus, alloys with both high strength and high chemical resistance may be considered for work under stress and aggressive environment at temperatures between 1100°C and almost 1250°C, thanks to efficiently reinforcing TaC particles and to available chromium leading to protective chromia scale. This latter might be subject to volatilization at so high temperatures, but it can also provide several improvements, as a better resistance against both oxidation by gases and corrosion by melts.

References

[1] M. A. Khan, N. R. Prasad, S. N. Krishnan, S. K. Raja, J. T. W. Jappes, M. Duraiselvam; Materials and Manufacturing Processes 32(14) (2017) 1635-1641.
[2] E. F. Bradley, Superalloys: A Technical Guide, ASM International, Metals Park, 1988.
[3] M. J. Donachie, S. J. Donachie, Superalloys: A Technical Guide, ASM International, Materials Park, 2002.
[4] A. Szczotok; Archives of Metallurgy and Materials 62(2) (2017) 581-586.
[5] B. Dubiel, I. Kalemba-Rec, A. Kruk, T. Moskalewicz, P. Indyka, S. Kac, A. Radziszewska, A. Kopia, K. Berent, M. Gajewska; Materials Characterization 131 (2017) 266-276.
[6] V. Caccuri, J. Cormier, R. Desmorat ; Materials&Design 131 (2017) 487-497.
[7] D.A. Bridgeport, W.A. Brandtley, P.F. Herman, Journal of Prosthodontics 2(3) (1993) 144-150.
[8] B.Roebuck, E.A.Almond; International Materials Reviews 33 (1988) 90-110.
[9] C. T. Sims, W. C. Hagel, The Superalloys, John Wiley & Sons, New York, 1972.
[10] P. Berthod, J.L. Bernard, C. Liébaut; Patent WO99/16919.
[11] N. C. Ritter, E. Schesler, A. Mueller, R. Retting, C. Koerner, R. F. Singer; Advanced Engineering Materials 19(8) (2017) DOI:10.1002/adem.201700150
[12] D. Young, High Temperature Oxidation and Corrosion of Metals, Elsevier Corrosion Series, Oxford, 2008.
[13] W. Ren, F. Ouyang, B. Ding, Y. Zhong, J. Yu, Z. Ren, L. Zhou; Journal of Alloys and Compounds 724 (2017) 565-574.
[14] S. Michon, P. Berthod, L. Aranda, C. Rapin, R. Podor, P. Steinmetz; Calphad 27(3) (2003) 289-294.
[15] P. Berthod, Y. Hamini, L. Aranda, L. Héricher; Calphad 31(3) (2007) 351-360.
[16] P. Berthod, L. Aranda, C. Vébert, S. Michon; Calphad 28(2) (2004) 159-166.
[17] P. Berthod, Y. Hamini, L. Héricher, L. Aranda; Calphad 31(3) (2007) 361-369.

Table 1
Chemical compositions of the studied alloys; *theoretic* and obtained*

	Ni	Co	Cr	Ta	C
5Ni0Co	*68.6*	*0*	*25*	*6*	*Expected 0.4wt.% for all alloys*
	Bal.	/	25.5 ±0.1	6.5 ±0.2	
4Ni1Co	*54.88*	*13.72*	*25*	*6*	
	Bal.	14.3 ±0.2	25.4 ±0.4	5.6 ±0.9	
3Ni2Co	*41.16*	*27.44*	*25*	*6*	
	Bal.	27.2 ±0.2	25.4 ±0.1	6.5 ±0.2	
2Ni3Co	*27.44*	*41.16*	*25*	*6*	
	25.4 ±0.3	Bal.	25.7 ±0.4	6.9 ±0.2	
1Ni4Co	*13.72*	*54.88*	*25*	*6*	
	12.7 ±0.5	Bal.	26.2 ±0.2	6.6 ±0.8	
0Ni5Co	*0*	*68.6*	*25*	*6*	
	/	Bal.	25.3 ±0.2	7.2 ±0.5	

*: average and standard deviation values from the SEM/BSE full frame measurements three randomly chosen ×250 areas

Table 2
Surface fractions of the tantalum carbides and of the chromium carbides present in the alloys in their different metallurgical states

Alloy designation	**Metallurgical state**	**Surf.% TaC**		**Surf.% Cr_xC_y**	
		average value	**standard deviation**	**average value**	**standard deviation**
5Ni0Co	*Aged @1237°C*	*2.9*	*±0.3*	*4.8*	*±1.7*
	Aged @1127°C	2.6	±0.2	4.0	±0.7
	As-cast	**1.3**	**±0.3**	**3.3**	**±0.5**
4Ni1Co	*Aged @1237°C*	*4.7*	*±0.1*	*3.1*	*±0.3*
	Aged @1127°C	5.8	±0.7	2.4	±0.8
	As-cast	**1.6**	**±0.0**	**1.2**	**±0.0**
3Ni2Co	*Aged @1237°C*	*5.8*	*±0.9*	*0.4*	*±0.3*
	Aged @1127°C	4.1	±0.2	0.9	±0.4
	As-cast	**3.8**	**±1.0**	**1.4**	**±0.3**
2Ni3Co	*Aged @1237°C*	*6.8*	*±0.9*	*0.1*	*±0.0*
	Aged @1127°C	5.7	±0.4	0.1	±0.1
	As-cast	**6.8**	**±1.0**	**0.1**	**±0.0**
1Ni4Co	*Aged @1237°C*	*7.2*	*±0.1*	*0.0*	*±0.0*
	Aged @1127°C	3.5	±0.7	0.0	±0.0
	As-cast	**5.6**	**±2.2**	**0.0**	**±0.0**
0Ni5Co	*Aged @1237°C*	*7.0*	*±0.8*	*0.0*	*±0.0*
	Aged @1127°C	4.7	±0.7	0.0	±0.0
	As-cast	**6.2**	**±1.4**	**0.2**	**±0.2**

Table 3
Hardness of the alloys in their different metallurgical states

Alloy designation	Metallurgical state	Hardness / Hv_{10kg}	
		average value	standard deviation
5Ni0Co	*Aged @1237°C*	179	3
	Aged @1127°C	193	4
	As-cast	205	4
4Ni1Co	*Aged @1237°C*	184	3
	Aged @1127°C	204	4
	As-cast	196	9
3Ni2Co	*Aged @1237°C*	202	5
	Aged @1127°C	223	3
	As-cast	199	9
2Ni3Co	*Aged @1237°C*	218	5
	Aged @1127°C	270	4
	As-cast	260	3
1Ni4Co	*Aged @1237°C*	270	5
	Aged @1127°C	299	3
	As-cast	296	7
0Ni5Co	*Aged @1237°C*	306	6
	Aged @1127°C	337	5
	As-cast	339	7

Table 4
Thickness of the external oxide scales and depth of the carbide-free zones after oxidation for 24 hours at 1127°C or at 1237°C

Alloy designation	Temperature of oxidation	Scale thickness (µm)		Carbide-free depth (µm)	
		average value	standard deviation	average value	standard deviation
5Ni0Co	*1237°C*	/	/	*128*	*±8*
	1127°C	5.9	±1.6	28	±3
4Ni1Co	*1237°C*	*17*	*±6*	*98*	*±8*
	1127°C	6.0	±2.3	18	±5
3Ni2Co	*1237°C*	/	/	*85*	*±5*
	1127°C	4.9	±0.7	19	±2
2Ni3Co	*1237°C*	*21*	*±4*	*88*	*±10*
	1127°C	16	±4	42	±7
1Ni4Co	*1237°C*	//	//	*90*	*±12*
	1127°C	24	±5	36	±8
0Ni5Co	*1237°C*	//	//	*84*	*±7*
	1127°C	//	//	29	±6

/: oxide scale spalled off //: oxide scale not regular

Table 5
Chromium content in ally very close to the oxidation front after oxidation for 24h at 1127°C or 1237°C

Alloy designation	**Metallurgical state**	**Chromium content in extreme surface (µm)**	
		average value	**standard deviation**
5Ni0Co	*1237°C* 1127°C	*19.8* 16.8	*±0.3* ±0.6
4Ni1Co	*1237°C* 1127°C	*19.6* 16.9	*±0.1* ±0.1
3Ni2Co	*1237°C* 1127°C	*17.7* 16.1	*±0.5* ±0.4
2Ni3Co	*1237°C* 1127°C	*17.5* 13.0	*±0.2* ±3.3
1Ni4Co	*1237°C* 1127°C	*11.0* 13.1	*±0.4* ±0.3
0Ni5Co	*1237°C* 1127°C	*10.6* 12.4	*±1.0* ±0.3

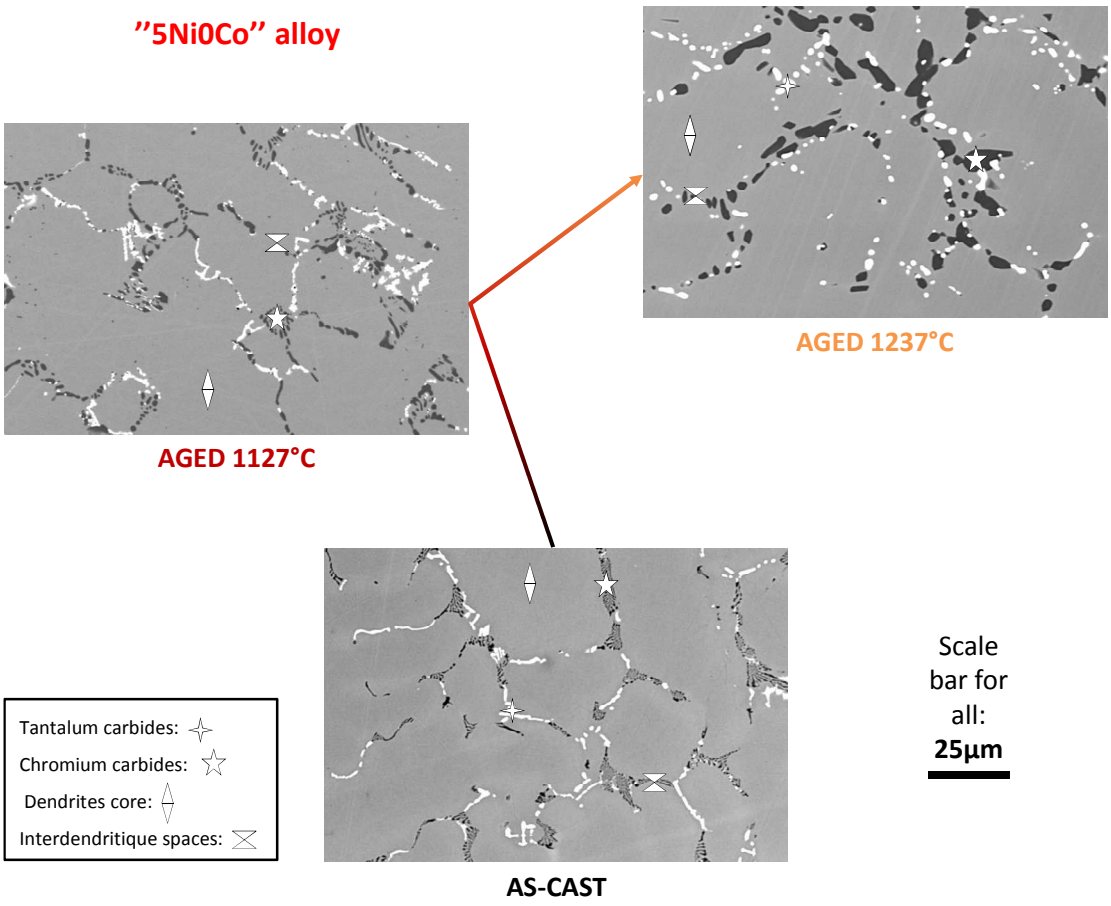

Fig. 1.
SEM/BSE micrographs illustrating the as-cast (bottom), 1127°C-24h aged (middle position) and 1237°C-24h aged (top) microstructures of the "5Ni0Co" alloy

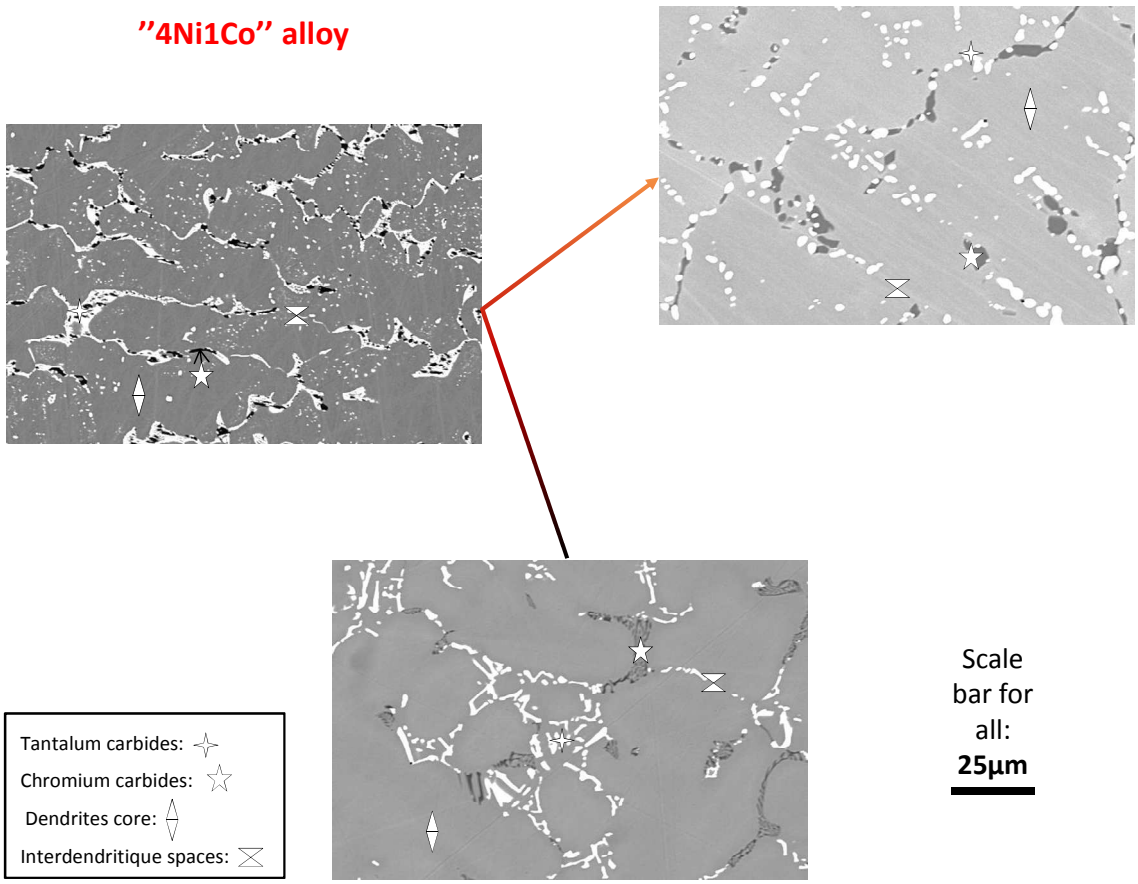

Fig. 2.
SEM/BSE micrographs illustrating the as-cast (bottom), 1127°C-24h aged (middle position) and 1237°C-24h aged (top) microstructures of the "4Ni1Co" alloy

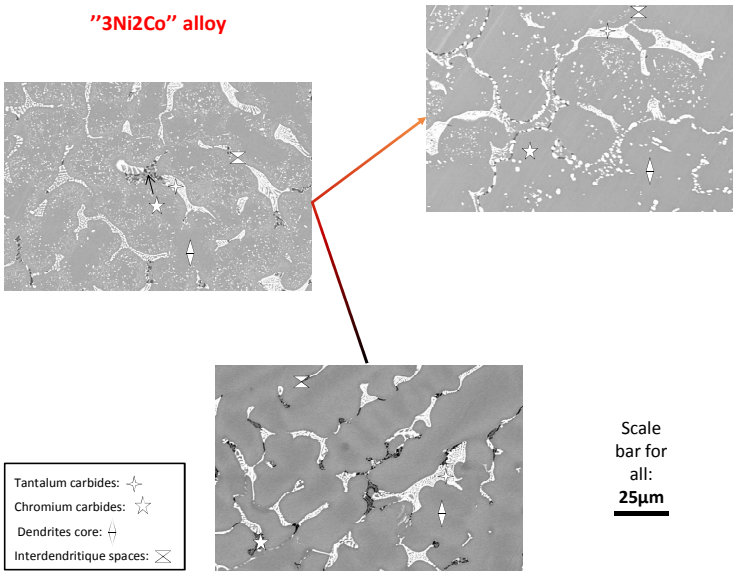

Fig. 3.
SEM/BSE micrographs illustrating the as-cast (bottom), 1127°C-24h aged (middle position) and 1237°C-24h aged (top) microstructures of the “3Ni2Co” alloy

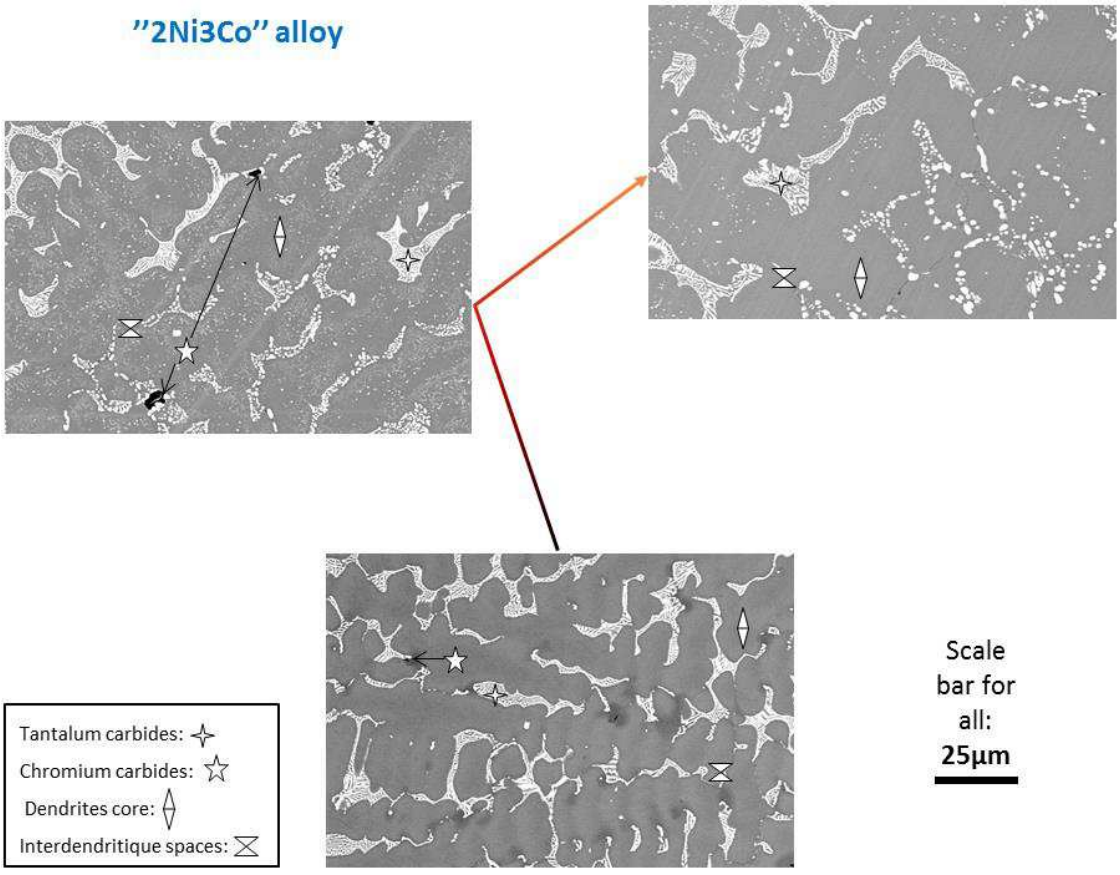

Fig. 4.
SEM/BSE micrographs illustrating the as-cast (bottom), 1127°C-24h aged (middle position) and 1237°C-24h aged (top) microstructures of the "2Ni3Co" alloy

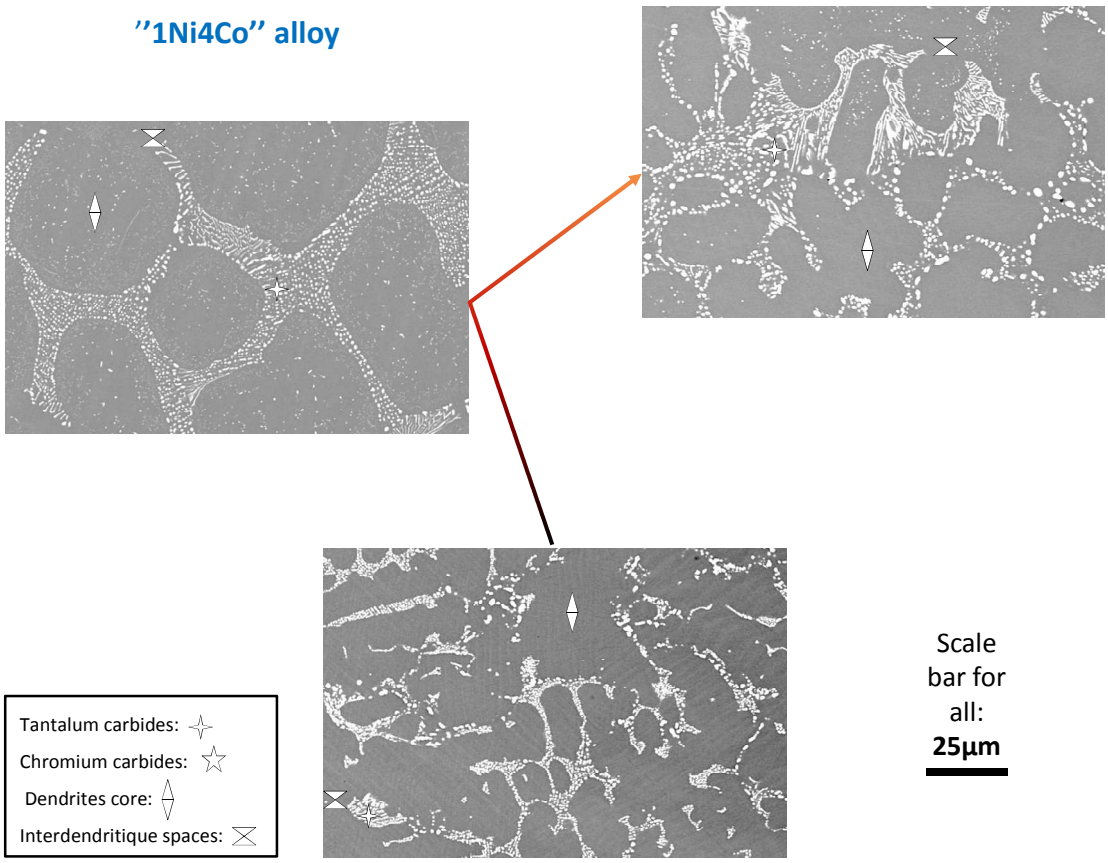

Fig. 5.
SEM/BSE micrographs illustrating the as-cast (bottom), 1127°C-24h aged (middle position) and 1237°C-24h aged (top) microstructures of the "1Ni4Co" alloy

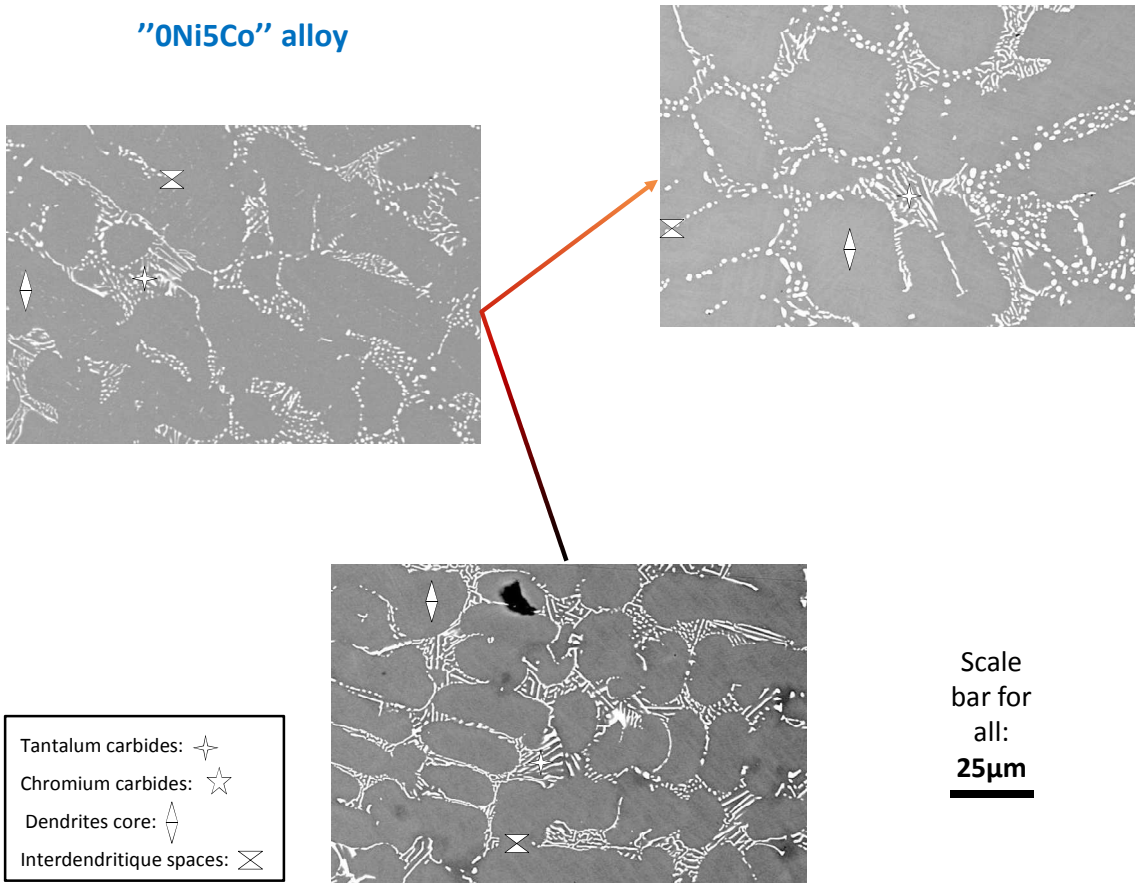

Fig. 6.
SEM/BSE micrographs illustrating the as-cast (bottom), 1127°C-24h aged (middle position) and 1237°C-24h aged (top) microstructures of the “0Ni5Co” alloy

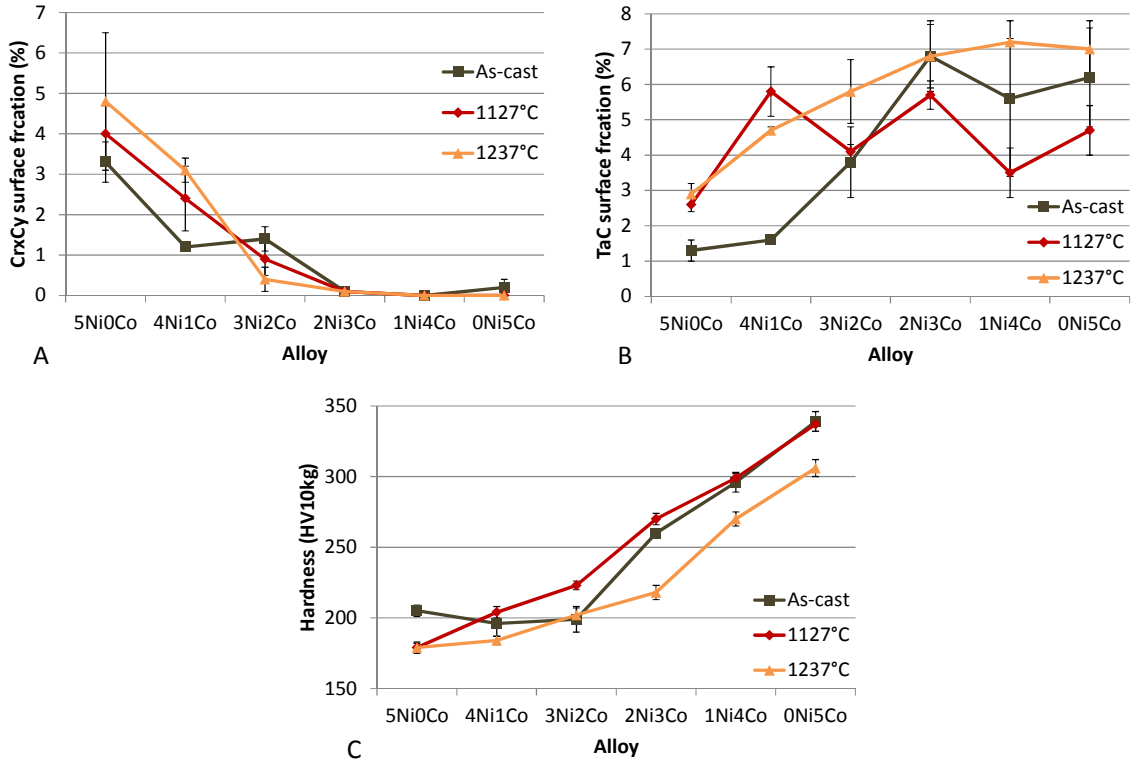

Fig. 7.
Evolution, with the cobalt content, of the surface fraction of chromium carbides (A), of the surface fraction of the tantalum carbides (B) and of the hardness (C), for the three metallurgical states (as-cast, aged 24h at 1127°C, aged 24h at 1237°C)

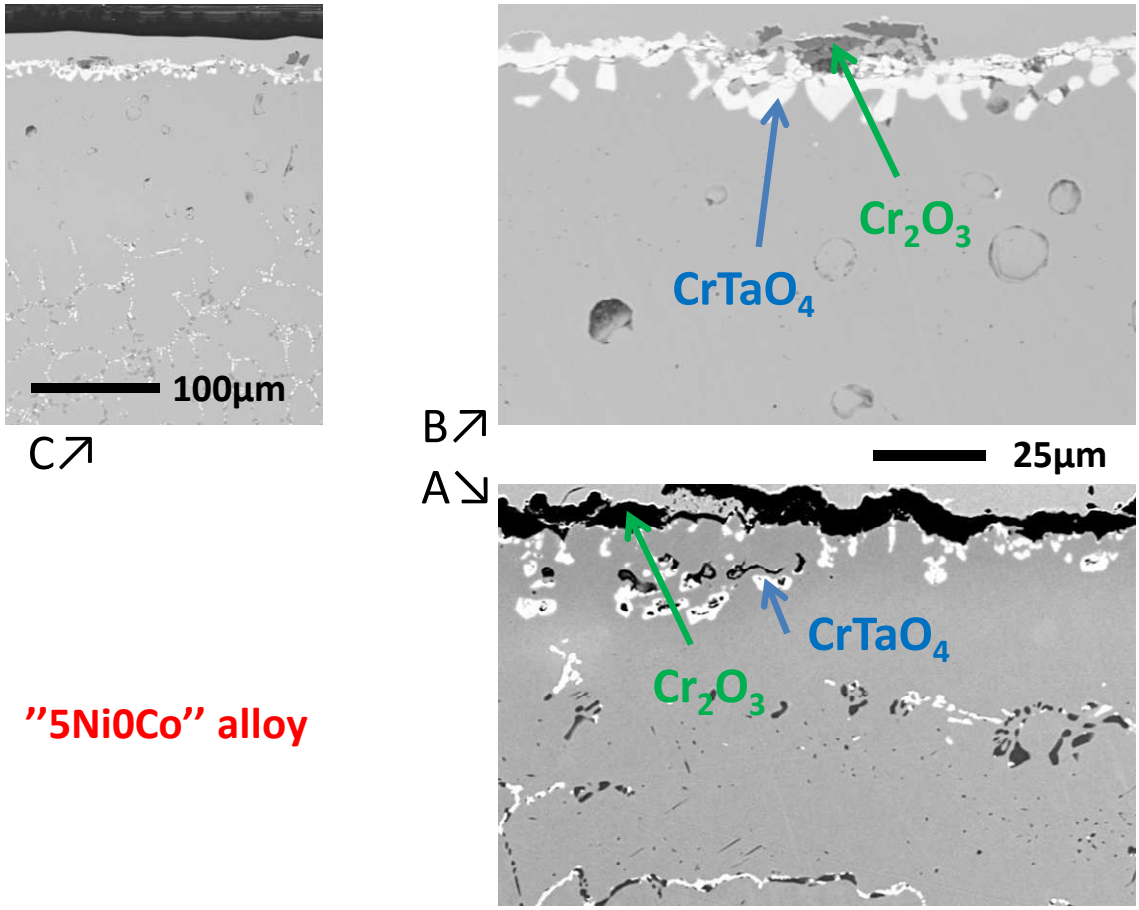

Fig. 8.
SEM/BSE micrographs illustrating the surface (A, B) and subsurface (A, C) deteriorations of the "5Ni0Co" alloy after 24 hours spent at 1127°C (A) or 1237°C (B & C) in hot laboratory air

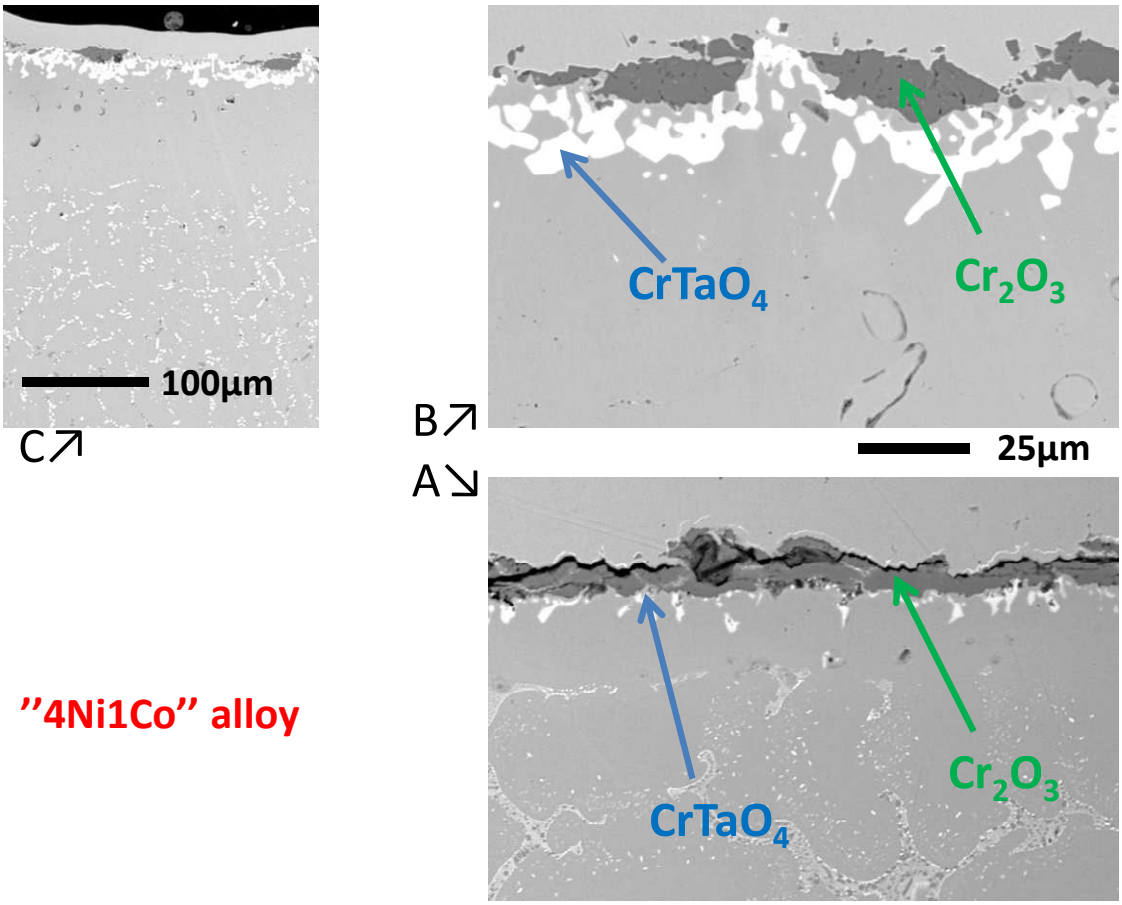

Fig. 9.
SEM/BSE micrographs illustrating the surface (A, B) and subsurface (A, C) deteriorations of the "4Ni1Co" alloy after 24 hours spent at 1127°C (A) or 1237°C (B & C) in hot laboratory air

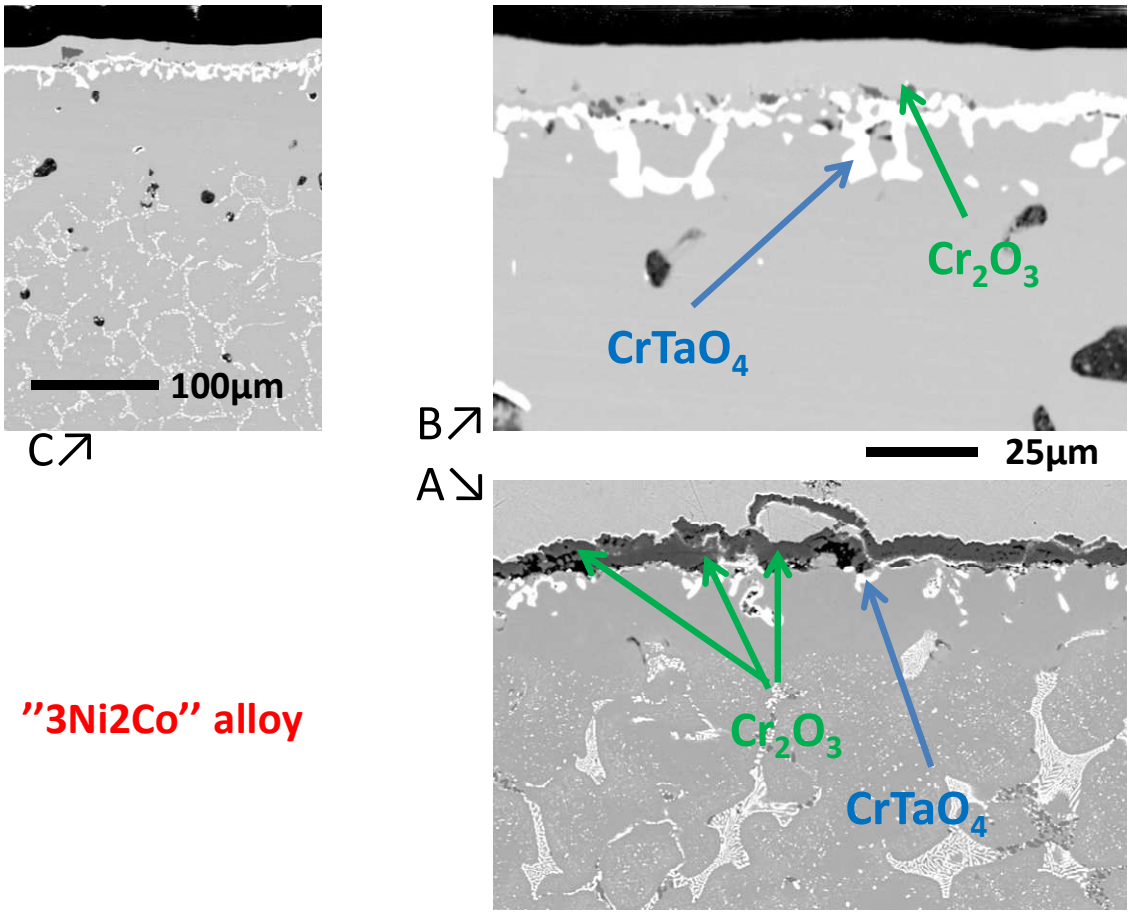

Fig. 10.
SEM/BSE micrographs illustrating the surface (A, B) and subsurface (A, C) deteriorations of the "3Ni2Co" alloy after 24 hours spent at 1127°C (A) or 1237°C (B & C) in hot laboratory air

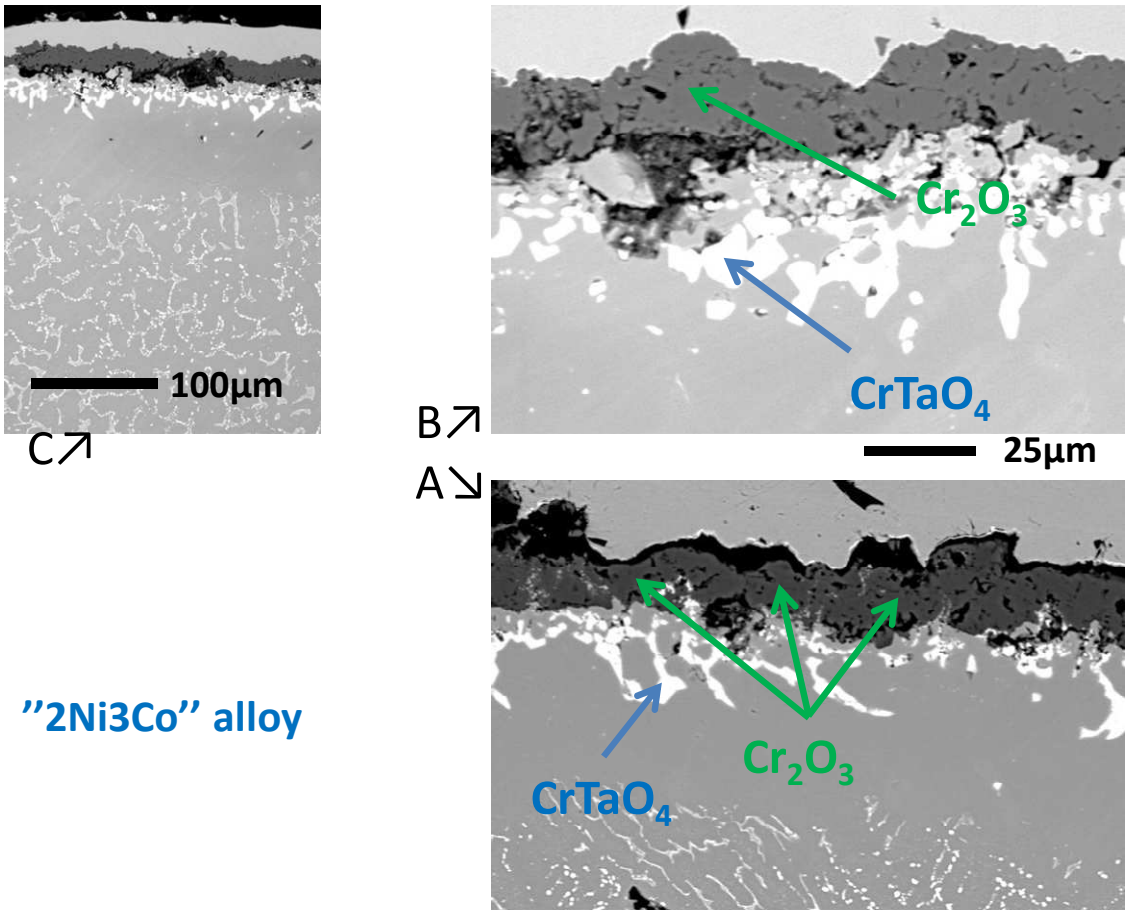

Fig. 11.
SEM/BSE micrographs illustrating the surface (A, B) and subsurface (A, C) deteriorations of the "2Ni3Co" alloy after 24 hours spent at 1127°C (A) or 1237°C (B & C) in hot laboratory air

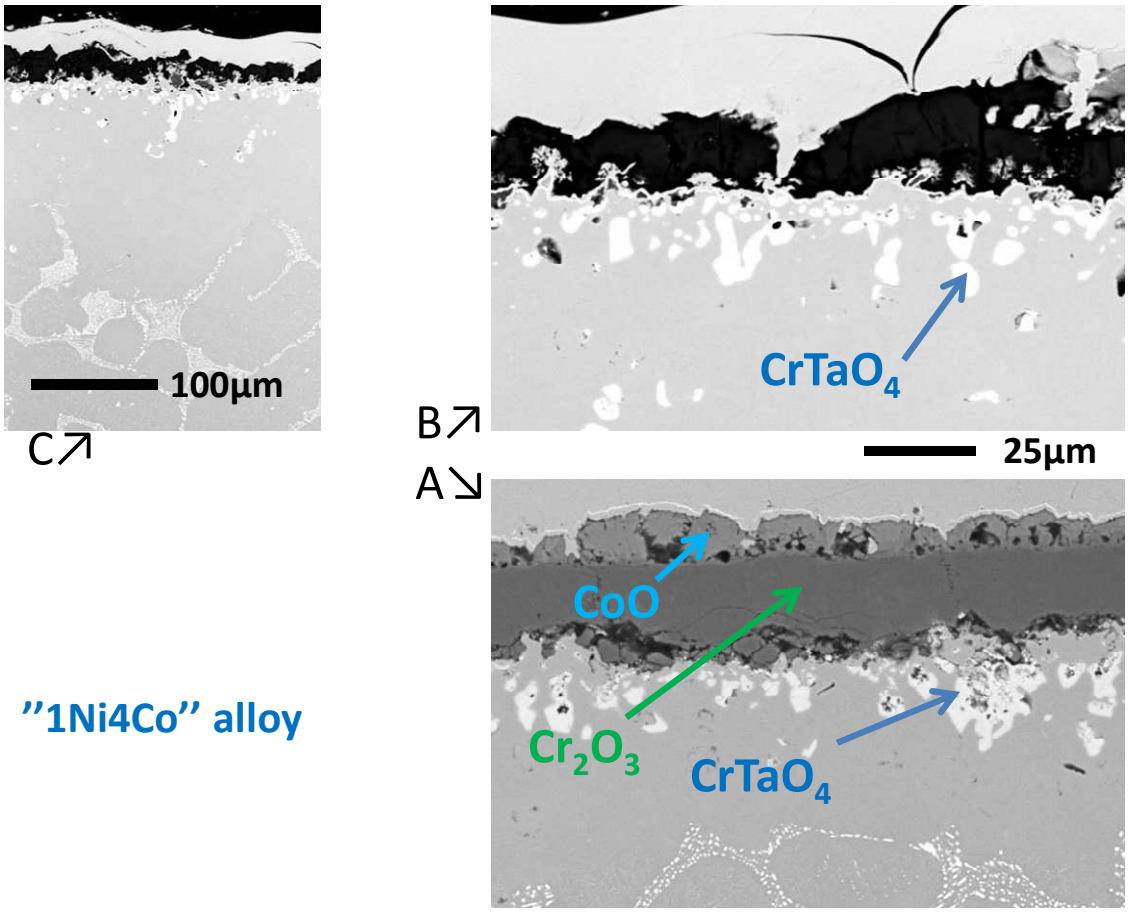

Fig. 12.
SEM/BSE micrographs illustrating the surface (A, B) and subsurface (A, C) deteriorations of the “1Ni4Co” alloy after 24 hours spent at 1127°C (A) or 1237°C (B & C) in hot laboratory air

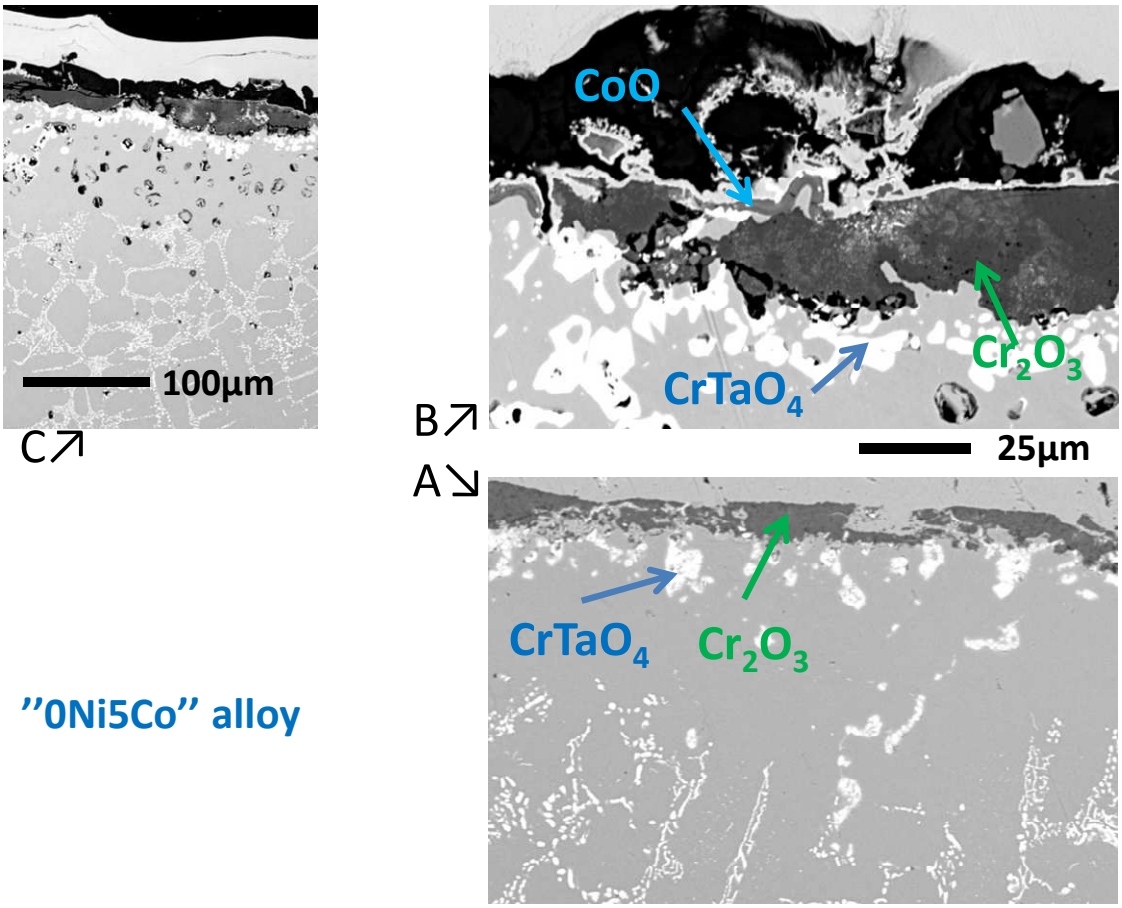

Fig. 13.
SEM/BSE micrographs illustrating the surface (A, B) and subsurface (A, C) deteriorations of the "0Ni5Co" alloy after 24 hours spent at 1127°C (A) or 1237°C (B & C) in hot laboratory air

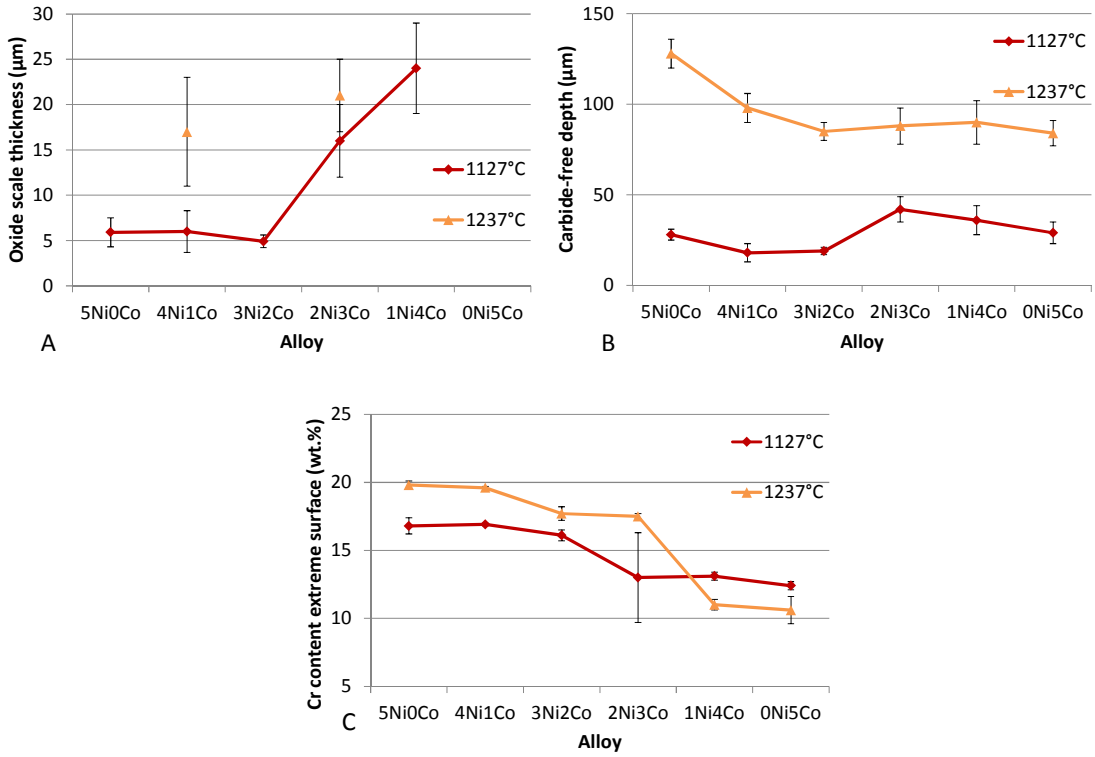

Fig. 14.
Evolution, with the cobalt content, of the thickness of the external oxide scale (A), of the depth of the carbide-free zone (B) and of the chromium content in extreme surface (C), for the two oxidized states (after 24h of aging at 1127°C, after 24h of aging at 1237°C)